International Journal of Bifurcation and Chaos, Vol. 14, No. 7 (2004) 2341–2351

DYNAMICS OF PIECEWISE LINEAR DISCONTINUOUS MAPS

LÁSZLÓ E. KOLLÁR
Department of Applied Sciences, University of Québec at Chicoutimi,
555, Boul. de l'Université, Chicoutimi, Québec G7H 2B1, Canada
laszlo_kollar@uqac.ca

GÁBOR STÉPÁN*
Department of Applied Mechanics, Budapest University of Technology and Economics
Budapest H-1521, Hungary
stepan@mm.bme.hu

JÁNOS TURI
Department of Mathematical Sciences, The University of Texas at Dallas,
P. O. Box 830688, M/S EC 35, Richardson, TX 75083-0688, USA
turi@utdallas.edu

Received September 25, 2002; Revised April 10, 2003

In this paper, the dynamics of maps representing classes of controlled sampled systems with backlash are examined. First, a bilinear one-dimensional map is considered, and the analysis shows that, depending on the value of the control parameter, all orbits originating in an attractive set are either periodic or dense on the attractor. Moreover, the dense orbits have sensitive dependence on initial data, but behave rather regularly, i.e. they have quasiperiodic subsequences and the Lyapunov exponent of every orbit is zero. The inclusion of a second parameter, the processing delay, in the model leads to a piecewise linear two-dimensional map. The dynamics of this map are studied using numerical simulations which indicate similar behavior as in the one-dimensional case.

Keywords: Sampling; process delay; backlash; weak chaos.

1. Preliminaries

We consider the map

$$x_{j+1} = Ax_j - B\Phi(x_j)\,, \quad j = 0, 1, 2, \ldots, \tag{1}$$

with the initial condition x_0 and

$$\Phi(x_j) = \begin{cases} 0\,, & |x_j| < 1 \\ x_j\,, & |x_j| \geq 1\,, \end{cases}$$

in the parameter domain $A > 1$, $|A - B| < 1$. Such maps naturally arise in digitally controlled mechanical systems [Kollár *et al.*, 2003; Lóránt & Stépán, 1996; Theodossides & Natsiavas, 2000].

Remark 1.1. This map can be obtained by discretizing the following differential equation with piecewise constant on right-hand side [Kollár, 2001]

$$\begin{gathered}\dot{\tilde{x}}(t) - a\tilde{x}(t) = -P\tilde{\psi}(\tilde{x}(j\tau))\tilde{x}(j\tau)\,, \\ t \in [j\tau, (j+1)\tau)\,, \quad j = 0, 1, 2, \ldots,\end{gathered} \tag{2}$$

*Author for correspondance.

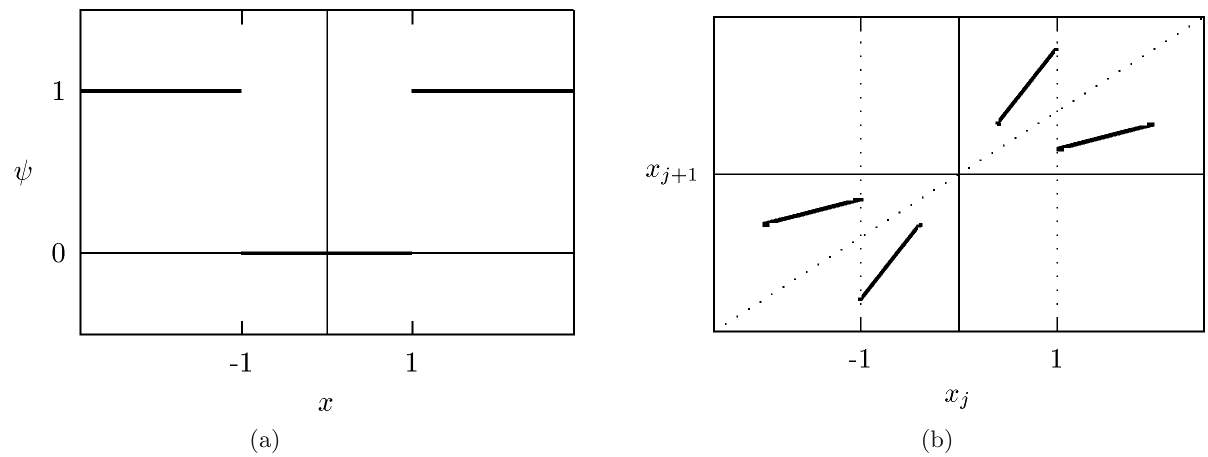

Fig. 1. (a) The piecewise constant function ψ. (b) The discrete one-dimensional map.

where $a > 0$, the sampling rate $\tau > 0$, and the control parameter $P > 0$. The function $\tilde{\psi}$ is given by

$$\tilde{\psi}(\tilde{x}(j\tau)) = \begin{cases} 0\,, & |\tilde{x}(j\tau)| < \delta \\ 1\,, & |\tilde{x}(j\tau)| \geq \delta \end{cases}, \quad \delta > 0\,. \tag{3}$$

Note that (2) and (3) represent a controlled linear system with backlash (i.e. the control can only act outside a δ neighborhood of the equilibrium).

For convenience, we introduce the rescalings $x = \tilde{x}/\delta$ and $T = t/\tau$. Then we consider the function ψ

$$\psi(x(j)) = \tilde{\psi}(\tilde{x}(j\tau)) = \begin{cases} 0\,, & |x(j)| < 1 \\ 1\,, & |x(j)| \geq 1\,, \end{cases} \tag{4}$$

that is shown in Fig. 1(a), and obtain an equivalent equation

$$\begin{aligned} x'(T) - a\tau x(T) &= -P\tau\psi(x(j))x(j)\,, \\ T \in [j,\, j+1)\,, &\quad j = 0,\, 1,\, 2, \ldots, \end{aligned} \tag{5}$$

where $' = d/dT$. The general solution of this equation on the interval $[j,\, j+1)$ can be obtained by the variation of constants formula as follows

$$x(T) = \mathrm{e}^{a\tau(T-j)}x(j) + \int_j^{j+1} \mathrm{e}^{a\tau(T-s)}(-P)\tau\psi(x(j))x(j)\mathrm{d}s\,.$$

Substituting $T = j + 1$, introducing the notation $x_j = x(j)$, and evaluating the resulting integral yield the one-dimensional map

$$x_{j+1} = \left[\mathrm{e}^{a\tau} + (1 - \mathrm{e}^{a\tau})\frac{P}{a}\,\psi(x_j)\right] x_j\,. \tag{6}$$

Introduce the notation

$$\begin{aligned} A = \mathrm{e}^{a\tau}, \quad B &= -(1 - \mathrm{e}^{a\tau})\frac{P}{a}\,, \\ \Phi(x_j) &= \psi(x_j)x_j\,, \end{aligned} \tag{7}$$

then the map (6) can be written in the form of (1). This map is depicted in Fig. 1(b).

Example 1.2. Equation (2) can describe a one-degree-of-freedom mechanical system under the effect of velocity-dependent forces. Since the controlled variable is the velocity, the governing equation is a first-order differential equation with piecewise constant as right-hand side where the variable $\tilde{x}$ is the velocity. This equation arises, e.g. in the study of stick-and-slip motion of certain machine tool parts. For these systems digital control can be used to achieve a stable, small feed rate of the tool [Haller & Stépán, 1996].

Remark 1.3. If $\Phi(x_j) \equiv x_j$ (i.e. no backlash), then the fixed point 0 is asymptotically stable if and only if $|A - B| < 1$ or, equivalently, $a < P < a(\mathrm{e}^{a\tau} + 1)/(\mathrm{e}^{a\tau} - 1)$.

Remark 1.4. The orbits of the map (1) represent discrete points of the trajectories of the scaled differential equation (5) in the neighborhood of unstable equilibrium $x = 0$.

Remark 1.5. Equation (7) describes a one-to-one relationship between P and B. For convenience, in the next section, we state our results with parameter B instead of parameter P.

2. Statements of the Main Results

In this section we analyze the behavior of the orbits of the map (1) depending on the parameter B. Although $x = 0$ equilibrium is unstable, we can find invariant sets for every choice of B which attracts every orbit except the trivial one (i.e. $x_n \equiv 0$). If $A - B > 0$ then this set is $[A - B, A)$ or $(-A, -(A - B)]$ if $x_0 > 0$ or $x_0 < 0$, respectively. If $A - B < 0$ then this set is $(-A, -(A - B)] \cup [A - B, A)$. When $A - B > 0$, the cases $x_0 > 0$ and $x_0 < 0$ are symmetric, therefore it is enough to examine the case $x_0 > 0$ without loss of generality. When $A - B < 0$, $|x_n|$ coincides with the nth iterate of a positive x_0 of the map $x_{j+1} = |A - B|x_j$, hence the case $A - B > 0$ can be extended easily for the case $A - B < 0$. In what follows, we discuss the case $A - B > 0$, $x_0 > 0$ and we denote the invariant set $[A - B, A)$ by $\mathcal{A}$. The behavior of orbits depends on B. There are two possibilities:

(i) every orbit is eventually periodic or,
(ii) every orbit is dense.

Next, we give a necessary and sufficient condition for the existence of periodic orbits.

Theorem 2.1. *Let $x_0 \in \mathcal{A}$. Then the orbit originating in x_0 is periodic if and only if B satisfies the condition*

$$B = A - \frac{1}{\sqrt[n-k]{A^k}}\,, \tag{8}$$

where $k, n \in \mathbb{Z}$, $n \geq 2$, $1 \leq k \leq n-1$ and n is the period.

Proof. First, prove that if a period-n orbit exists then the condition of the theorem holds. Consider a period-n orbit. Let x_0 be a point of this periodic orbit. Then

$$x_n = A^k(A-B)^{n-k}x_0\,,$$

if the periodic orbit has k points in the interval $[A - B, 1)$ and $n - k$ points in the interval $[1, A)$. Since the orbit is a period-n orbit, $x_n = x_0$, and we have $A^k(A - B)^{n-k} = 1$. This relation implies the formula given in the theorem.

Now, suppose that

$$B = A - \frac{1}{\sqrt[n-k]{A^k}}\,,$$

where $k, n \in \mathbb{Z}$, $n \geq 2$, $1 \leq k \leq n-1$, and show that a period-n orbit exists. This equality implies that $A^k(A-B)^{n-k} = 1$. Consider the following process. Choose an initial value x_0 in the attractor and multiply it by A if $x_0 < 1$ or by $A - B$ if $x_0 \geq 1$, and remove an A or an $A - B$ from the product $A^k(A - B)^{n-k}$. Then show that the process can be continued, i.e. the new product contains A if $x_1 < 1$ or $A - B$ if $x_1 \geq 1$, and this holds for each $m \in \mathbb{Z}$ if $m < n$.

Assume that $A - B \leq x_0 < 1$. Then $x_1 = Ax_0$ and the product $A^k(A - B)^{n-k}$ certainly contains A, because $k \geq 1$. Now suppose that this process is continued for m steps and $x_m = A^l(A - B)^{m-l}$, where $l \in \mathbb{Z}$, $l \leq k$ and $m - l \leq n - k$, but at most one equality holds, so $m < n$. Otherwise, $m = n$ and $x_m = x_n = A^k(A - B)^{n-k}x_0 = x_0$, so the period-$n$ orbit is found. We consider the following three cases.

(i) $1 \leq x_m < A$
This implies that $A^l(A - B)^{m-l} > 1$ and the new product $A^{k-l}(A - B)^{n-k-(m-l)}$ is strictly less than 1. The new product must contain $A - B$, so the process can be continued.
(ii) $A - B \leq x_m \leq x_0$ (but $m < n$)
This implies that $A^l(A - B)^{m-l} \leq 1$ and the new product $A^{k-l}(A - B)^{n-k-(m-l)}$ is greater than or equal to 1. The new product must contain A, so the process can be continued.
(iii) $x_0 < x_m < 1$
Recall that $A - B \leq x_0$. After multiplying both sides of this relation by $A^l(A - B)^{m-l}$, we have $(A - B)A^l(A - B)^{m-l} \leq x_m < 1$ and this implies that $A^l(A - B)^{m-l+1} < 1$. Since $A^l(A - B)^{m-l} > 1$, $m - l < n - k$ or $m - l + 1 \leq n - k$. Since $A^k(A - B)^{n-k} = 1$, it follows that $l < k$ and the process can be continued.

The case $1 \leq x_0 < A$ can be treated by using the same procedure. ■

Theorem 2.2. *Assume that B is chosen such that condition (8) is not satisfied. Then the orbits are dense on the attractor $\mathcal{A}$.*

Proof. We prove this theorem in three steps. First, the map is transformed to a logarithmic map. Then the motion is simplified to a motion on a circle in one direction. Finally, we show that points of an orbit are dense on the circle.

Let $b = \ln A$, $c = \ln(A - B)$ and $y_j = \ln x_j$, $j = 1, 2, \ldots,$ where $b > 0$ and $c < 0$. Then we obtain the following map

$$y_{j+1} = \begin{cases} b + y_j\,, & y_j < 0 \\ c + y_j\,, & y_j \geq 0\,. \end{cases}$$

If periodic solutions do not exist, i.e. $x_i \neq x_j$ for all $i,\, j \in \mathbb{Z}^+$, $i \neq j$, then $A^k(A-B)^{n-k}$ is different from 1 for any $k,\, n \in \mathbb{Z}^+$ or $kb+(n-k)c$ is different from 0. It implies that b/c is not rational.

This map gives a motion in the interval $[c,\, b)$, where y_{j+1} could be both less and greater than y_j. Now this motion is transformed to a motion on a circle in one direction. Let $0 \leq y_0 < b$. First, assume that $-c > b$. Then $y_1 = c + y_0 < 0$. Let $m \in \mathbb{Z}^+$ such that $y_m = (m-1)b + c + y_0 \geq 0$, but $y_{m-1} < 0$. Suppose that $y_m < y_0$. Let $y_0 - y_m = d$ and let $l \in \mathbb{Z}^+$ such that $y_{lm} = l(m-1)b + lc + y_0 < 0$, but $y_{(l-1)m} \geq 0$. $y_{lm+1} \geq 0$, since $d < b$. If we consider the interval $[0,\, b)$ as a circle, then the distance between y_{lm+1} and $y_{(l-1)m}$ is d. Repeating these cycles with m or $m+1$ steps, we take steps on the circle in one direction with length d which provides a quasiperiodic subsequence of the orbit.

Now we show that an orbit can approach any point in the interval $[0,\, b)$ arbitrarily. The proof is similar for the interval $[c,\, 0)$. Since $d = y_0 - y_m = -(m-1)b - c$, it implies that $d/b = -(m-1) - c/b$. $m-1$ is rational and c/b is not rational, therefore d/b is not rational. Choose an arbitrary point y^* on the circle. Since any irrational number can be approximated arbitrary closely by rational numbers, we can find $\overline{k},\, \overline{n} \in \mathbb{Z}^+$ such that for all $\varepsilon > 0$, the distance between $y^* + \overline{n}b$ and $y_0 + \overline{k}d$ is less than ε, i.e. starting from y_0, we can approach an arbitrary $y^* \in [0,\, b)$ after $\overline{k}$ steps, if $\overline{k}$ is large enough.

Further cases can be proved by following the same procedure. ■

Next, we observe how nearby orbits behave, then the Lyapunov exponent is calculated.

Theorem 2.3. *Let x_0 and $\overline{x}_0$ be two different initial values in the set $\mathcal{A}$. Furthermore, assume that B does not satisfy condition (8), i.e. the orbits are dense on the attractor $\mathcal{A}$. Then there exists an $n \in \mathbb{Z}^+$ such that the nth iterate of x_0 and $\overline{x}_0$, i.e. x_n and $\overline{x}_n$, respectively, are on opposite sides of 1.*

Proof. Let $x_0, \overline{x}_0 \in \mathcal{A}$ and $x_0 - \overline{x}_0 = \varepsilon$, where $\varepsilon > 0$. If x_0 and $\overline{x}_0$, or x_j and $\overline{x}_j$ for some $j \in \mathbb{Z}^+$ are on opposite sides of 1 then the theorem is proved. Now, suppose that x_j and $\overline{x}_j$ are on the same side of 1 for every $j \in \mathbb{Z}^+ \cup \{0\}$ and we show that it leads to contradiction. Let the nth iterate of x_0 be $x_n = K_n x_0$. Since x_j and $\overline{x}_j$ are on the same side of 1 for every $j \in \mathbb{Z}^+ \cup \{0\}$, they are always multiplied by the same number, therefore

$$\overline{x}_n = K_n \overline{x}_0 = K_n(x_0 - \varepsilon) = K_n x_0 - K_n \varepsilon\,. \tag{9}$$

The orbits are dense, therefore they approach 1 arbitrarily, i.e. for every $\delta > 0$ there exists an $n \in \mathbb{Z}^+$ such that

$$1 < x_n = K_n x_0 < 1 + \delta\,, \tag{10}$$

where δ is an arbitrary positive number, so it can be chosen such that $0 < \delta < \varepsilon/x_0$. By (10) we have

$$K_n \varepsilon > \frac{\varepsilon}{x_0} > \delta\,. \tag{11}$$

Then we obtain from (9)–(11) that

$$\overline{x}_n = K_n x_0 - K_n \varepsilon < K_n x_0 - \delta < 1\,,$$

i.e. x_n and $\overline{x}_n$ are on opposite sides of 1 which contradicts the assumption and proves the theorem. ■

Remark 2.4. Once two orbits are on opposite sides of 1, they are multiplied by different numbers and they leave each other's neighborhood.

Remark 2.5. The map $\mathbf{F} : \mathcal{A} \to \mathcal{A}$ is said to have sensitive dependence on initial conditions on $\mathcal{A}$ if there exists $\delta > 0$ such that, for any $\mathbf{x} \in \mathcal{A}$ and any neighborhood $U_{\mathbf{x}}$ of $\mathbf{x}$, there exists an $\overline{\mathbf{x}} \in U_{\mathbf{x}}$ and a positive integer n such that $|\mathbf{F}^n(\overline{\mathbf{x}}) - \mathbf{F}^n(\mathbf{x})| > \delta$ (see e.g. [Devaney, 1989; Wiggins, 1990]). Theorem 2.3 and Remark 2.4 imply that if B does not satisfy condition (8) then the map (1) has sensitive dependence on initial conditions on $\mathcal{A}$.

Remark 2.6. Although map (1) has sensitive dependence on initial conditions on $\mathcal{A}$, the motion is not unpredictable, because nearby orbits leave each other's neighborhood for one step only.

In the following, the Lyapunov exponent is computed. The Lyapunov exponent describes the behavior of nearby orbits. If nearby orbits attract each other, then the Lyapunov exponent is negative. If nearby orbits stretch each other exponentially then the Lyapunov exponent is positive.

Theorem 2.7. *The Lyapunov exponent of any orbit of map (1) is 0.*

Proof. If periodic orbits exist then every orbit is eventually periodic, therefore the Lyapunov exponents of periodic orbits are 0. To obtain the Lyapunov exponents of dense orbits, we determine the distribution function above the attractor. Let p_1 and p_2 be the probabilities of points of a trajectory in the interval $[A-B, 1)$ and $[1, A)$, respectively. The Lyapunov exponent can be calculated by applying the Frobenius–Perron equation [Szépfalusy & Tél, 1982]

$$\begin{aligned}\overline{\lambda} &= \int_0^1 P(x)\,\ln|F'(x)|\mathrm{d}x \\ &= p_1\ln A + p_2\ln(A-B)\,,\end{aligned} \tag{12}$$

since $F'(x) = A$ if $|x| < 1$ and $F'(x) = A - B$ if $|x| \geq 1$. The areas under the distribution function in the interval $[A-B, 1)$ and $[1, A)$, divided by the sum of the area under the distribution function in the attractor gives the probabilities p_1 and p_2, respectively. They are substituted into (12) and the Lyapunov exponent is determined. Since

$$P(x_{j+1}) = \sum_{j=1}^{n}\frac{P(x_j)}{|F'(x_j)|}$$

holds for the probability densities [Collet & Eckmann, 1980; Szépfalusy & Tél, 1982], it implies that

$$P(x_{j+1}) = P(Ax_j) = \frac{P(x_j)}{A}\,, \quad A(A-B) \leq x_{j+1} < A$$

$$P(x_{j+1}) = P((A-B)x_j) = \frac{P(x_j)}{A-B}\,, \quad A-B \leq x_{j+1} < A(A-B)\,.$$

$P(x) = c/x$ satisfies these equations in both intervals. Thus, it follows for the probabilities

$$p_1 = \int_{A-B}^{1}\frac{c}{x}\mathrm{d}x = -c\,\ln(A-B)\,,$$

$$p_2 = \int_{1}^{A}\frac{c}{x}\mathrm{d}x = c\,\ln A\,,$$

where

$$c = \frac{1}{\ln\dfrac{A}{A-B}}\,.$$

Substituting p_1 and p_2 into (12), yields $\overline{\lambda} = 0$. ■

The Lyapunov exponent is 0 for every value of B. Trajectories neither attract nor stretch each other exponentially.

3. Modeling Processing Delay

In the model of the present section, processing delay (for calculating the control force) is included, stability conditions are determined and numerical results are shown. The processing delay is assumed less than the sampling delay.

Consider the map

$$x_{j+1} = Ax_j - C\Phi(x_j) + (C-B)\Phi(x_{j-1})\,, \quad j = 1, 2, \ldots, \tag{13}$$

with initial condition x_0, $x_1 = Ax_0$ and

$$\Phi(x_j) = \begin{cases} 0\,, & |x_j| < 1 \\ x_j\,, & |x_j| \geq 1\,, \end{cases}$$

or equivalently

$$x_{j+1} = \begin{cases} Ax_j\,, & |x_j| < 1 \quad \text{and} \quad |x_{j-1}| < 1 \\ (A-C)x_j\,, & |x_j| \geq 1 \quad \text{and} \quad |x_{j-1}| < 1 \\ Ax_j + (C-B)x_{j-1}\,, & |x_j| < 1 \quad \text{and} \quad |x_{j-1}| \geq 1 \\ (A-C)x_j + (C-B)x_{j-1}\,, & |x_j| \geq 1 \quad \text{and} \quad |x_{j-1}| \geq 1\,. \end{cases}$$

Similarly to the procedure shown in Sec. 1, this map can be derived from the differential equation (2) with a "new" right-hand side due to the processing delay

$$\dot{\tilde{x}}(t) - a\tilde{x}(t) = \begin{cases} -P\tilde{\psi}(\tilde{x}((j-1)\tau_s))\tilde{x}((j-1)\tau_s)\,, & t \in [j\tau_s, j\tau_s + \tau_p) \\ -P\tilde{\psi}(\tilde{x}(j\tau_s))\tilde{x}(j\tau_s)\,, & t \in [j\tau_s + \tau_p, (j+1)\tau_s) \end{cases}$$

where $j = 1, 2, \ldots, \tau_s$ and τ_p are the sampling and the processing delay, respectively, $0 \le \tau_p \le \tau_s$, and the function $\tilde{\psi}$ is given by (3) as τ is interchanged by τ_s. The response to the actual data taken at the last sampling is provided after the processing delay. It means that, in the time interval $[j\tau_s, j\tau_s + \tau_p)$, the control force is still determined by the previously sampled data (i.e. the data sampled at $t = (j-1)\tau_s$), while, for the rest of the time before the next sampling $[j\tau_s + \tau_p, (j+1)\tau_s)$, the control force is determined by the new sampled data (at $t = j\tau_s$). Note that in the first step we do not have previously sampled data, and this explains that $x_1 = Ax_0$ independently from the value of x_0.

Introducing the rescalings $x = \tilde{x}/\delta$ and $T = t/\tau_s$ as well as considering the function ψ in (4), we obtain the equivalent equation

$$x'(T) - a\tau_s x(T) = \begin{cases} -P\tau_s\psi(x(j-1))x(j-1)\,, & t \in [j,\, j+\tau_p/\tau_s) \\ -P\tau_s\psi(x(j))x(j)\,, & t \in [j+\tau_p/\tau_s,\, j+1) \end{cases} \tag{14}$$

where $' = d/dT$ as in Sec. 1. The general solution of Eq. (14) on the interval $[j,\, j+\tau_p/\tau_s)$ can be obtained by the variation of constants formula as follows

$$x(T) = \mathrm{e}^{a\tau_s(T-j)}x(j) + \int_j^{j+\tau_p/\tau_s} \mathrm{e}^{a\tau_s(T-s)}(-P)\tau_s\psi(x(j-1))x(j-1)\mathrm{d}s\,.$$

Substituting $T = j + \tau_p/\tau_s$ and evaluating the resulting integral give

$$x\left(j + \frac{\tau_p}{\tau_s}\right) = \mathrm{e}^{a\tau_p}x(j) + (1-\mathrm{e}^{a\tau_p})\frac{P}{a}\,\psi(x(j-1))x(j-1)\,. \tag{15}$$

The general solution of Eq. (14) on the interval $[j+\tau_p/\tau_s,\, j+1)$ can be written in the form

$$x(T) = \mathrm{e}^{a\tau_s(T-(j+\tau_p/\tau_s))}x\left(j+\frac{\tau_p}{\tau_s}\right) + \int_{j+\tau_p/\tau_s}^{j+1} \mathrm{e}^{a\tau_s(T-s)}(-P)\tau_s\psi(x(j))x(j)\mathrm{d}s\,.$$

Similarly, substituting $T = j+1$ and evaluating the integral yield

$$x(j+1) = \mathrm{e}^{a\tau_s(1-\tau_p/\tau_s)}x\left(j+\frac{\tau_p}{\tau_s}\right) + (1-\mathrm{e}^{a\tau_s(1-\tau_p/\tau_s)})\frac{P}{a}\,\psi(x(j))x(j)\,. \tag{16}$$

As Eq. (15) is substituted into Eq. (16) and the notation $x_j = x(j)$ is introduced, we obtain the following map

$$x_{j+1} = \left[\mathrm{e}^{a\tau_s} + (1-\mathrm{e}^{a(\tau_s-\tau_p)})\frac{P}{a}\,\psi(x_j)\right]x_j + \left[(\mathrm{e}^{a(\tau_s-\tau_p)} - \mathrm{e}^{a\tau_s})\frac{P}{a}\,\psi(x_{j-1})\right]x_{j-1}\,. \tag{17}$$

Introduce the notation

$$A = \mathrm{e}^{a\tau_s}\,,\quad B = -(1-\mathrm{e}^{a\tau_s})\frac{P}{a}\,, \qquad C = -(1-\mathrm{e}^{a(\tau_s-\tau_p)})\frac{P}{a}\,,\quad \Phi(x_j) = \psi(x_j)x_j\,, \tag{18}$$

then the map (17) can be simplified to the form of (13).

Remark 3.1. According to (18) there is a one-to-one relationship between parameters P and τ_p and B and C, and therefore we can use either P and τ_p or B and C.

Stability is examined when $\Phi(x_j) \equiv x_j$ (i.e. no backlash). Map (13) can be simplified in the following form

$$x_{j+1} = (A-C)x_j + (C-B)x_{j-1}\,, \quad j = 1, 2, \ldots, \tag{19}$$

and it has the characteristic equation

$$\lambda^2 - (A-C)\lambda - (C-B) = 0\,. \tag{20}$$

The $(0, 0)^T$ fixed point of (19) is asymptotically stable if and only if the characteristic roots λ_1 and λ_2 of (20) are in modulus less than one. These yield the following conditions: (i) $A-B < 1$, (ii) $C-B > -1$, (iii) $(C-B)-(A-C) < 1$, or, equivalently, by using (18) (i) $P > a$, (ii) $P < a/(\mathrm{e}^{a\tau_s} - \mathrm{e}^{a(\tau_s-\tau_p)})$, (iii) $P < a(\mathrm{e}^{a\tau_s}+1)/(2\mathrm{e}^{a(\tau_s-\tau_p)} - \mathrm{e}^{a\tau_s} - 1)$ if $2\mathrm{e}^{a(\tau_s-\tau_p)} - \mathrm{e}^{a\tau_s} - 1 > 0$.

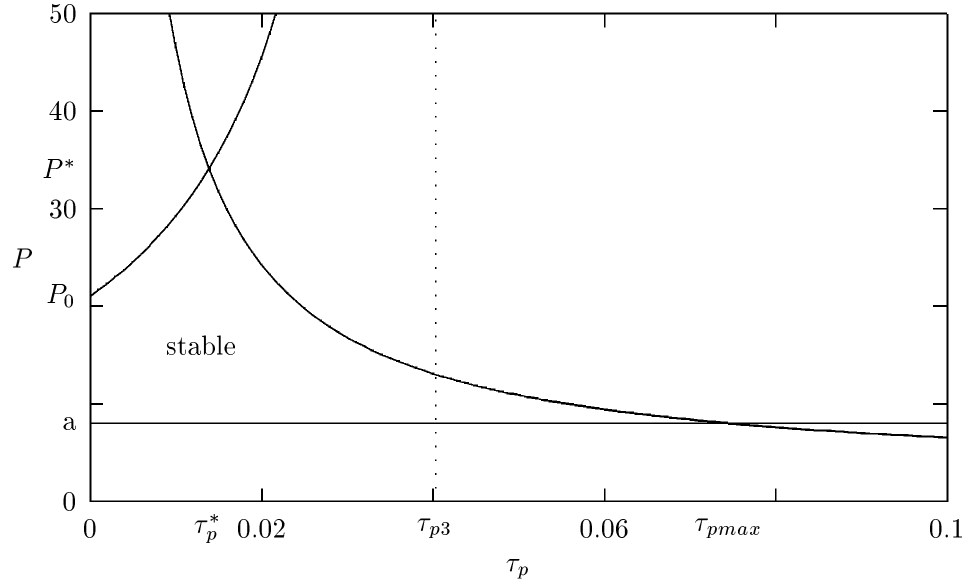

Fig. 2. The stability chart for $a = 8$ and $\tau_s = 0.1$.

The stability chart is constructed in the plane of τ_p and P for the following values of parameters: $a = 8$, $\tau_s = 0.1$ (see Fig. 2). Condition (i) gives a lower bound for P, while conditions (ii) and (iii) provide upper bounds for the control parameter. The P axis is the asymptote of condition (ii), and condition (iii) also has an asymptote at $\tau_{p3} = 2e^{a(\tau_s - \tau_p)} - e^{a\tau_s} - 1$, i.e. when the denominator in condition (iii) is 0. In spite of the asymptotes, P can never be arbitrarily large, because the curves intersect each other at

$$\tau_p^* = \frac{1}{a} \ln \frac{3e^{a\tau_s} + e^{2a\tau_s}}{e^{2a\tau_s} + 2e^{a\tau_s} + 1}.$$

This value can be obtained by equalizing conditions (ii) and (iii). Curves corresponding to conditions (i) and (iii) also intersect each other, so the maximal value τ_{pmax} of the processing delay, when successful control is possible, is given by equalizing these conditions

$$\tau_{\text{pmax}} = \frac{1}{a} \ln \frac{e^{a\tau_s}}{e^{a\tau_s} - 1}.$$

The assumption $\tau_p \leq \tau_s$ yields that the above τ_{pmax} exists only for $a \geq a_{\min} = (\ln 2)/\tau_s$. In particular, if $a = 8$ and $\tau_s = 0.1$, then $\tau_p^* = 0.0139$, $\tau_{p3} = 0.0403$, $a_{\min} = 6.9315$ and $\tau_{\text{pmax}} = 0.0746$. The value P_0 of the control parameter at $\tau_p = 0$ and the value P^* at $\tau_p = \tau_p^*$ can be obtained by subtituting $\tau_p = 0$ and $\tau_p = \tau_p^*$ into condition (iii): $P_0 = 21.06$, $P^* = 34.11$. It may be surprising that P can be larger if there is a small processing delay, but around the upper boundary of the stability domain the system is a bit overcontrolled and a small delay may improve stability.

In what follows let $\Phi(x_j) = \psi(x_j)x_j$. The following two sets of figures represent the effect of $\Phi(x_j)$ and the processing delay. Numerical results are shown for two different sets of parameters. In Fig. 3 parameters have the following values: $a = 10$, $P = 13.6788$ and $\tau_s = 0.1$. If $\tau_p = 0$ and $\Phi(x_j) \equiv x_j$ then the fixed point $(0, 0)^T$ is a stable node [see Fig. 3(a)]. For small enough τ_p, $(0, 0)^T$ is still stable, but it is a focus [see Fig. 3(b)]. For the rest of Fig. 3, $\Phi(x_j) = x_j$ and the line with tangent 1 is also shown. If $\tau_p = 0$ then this is a period-2 solution [see Fig. 3(c)]. In Figs. 3(d)–3(h), a set of numerical results can be seen as τ_p increases. In Fig. 3(h), $\tau_p = 0.0313$ which is the border of the stability domain. If $\tau_p > 0.0313$ then the motion is not stable for any initial condition. However, if the initial condition is small enough (e.g. $x_0 = 0.9$ in the figures), then the motion could be stable even if the processing delay is a bit larger than its value at the border of the stability domain. In Figs. 4(a)–4(g) the values of parameters are $a = 8$, $P = 10$ and $\tau_s = 0.1$. If $\Phi(x_j) \equiv x_j$ then $(0, 0)^T$ is a stable node or focus depending on the processing delay as in the previous case [see Figs. 4(a) and 4(b)]. For the rest of Fig. 4, $\Phi(x_j) = x_j$. If $\tau_p = 0$ then this is a nonperiodic solution [see Fig. 4(c)]. In Figs. 4(d)–4(g), we can again see how irregular motions are obtained as τ_p increases. In Fig. 4(h), we chose parameters

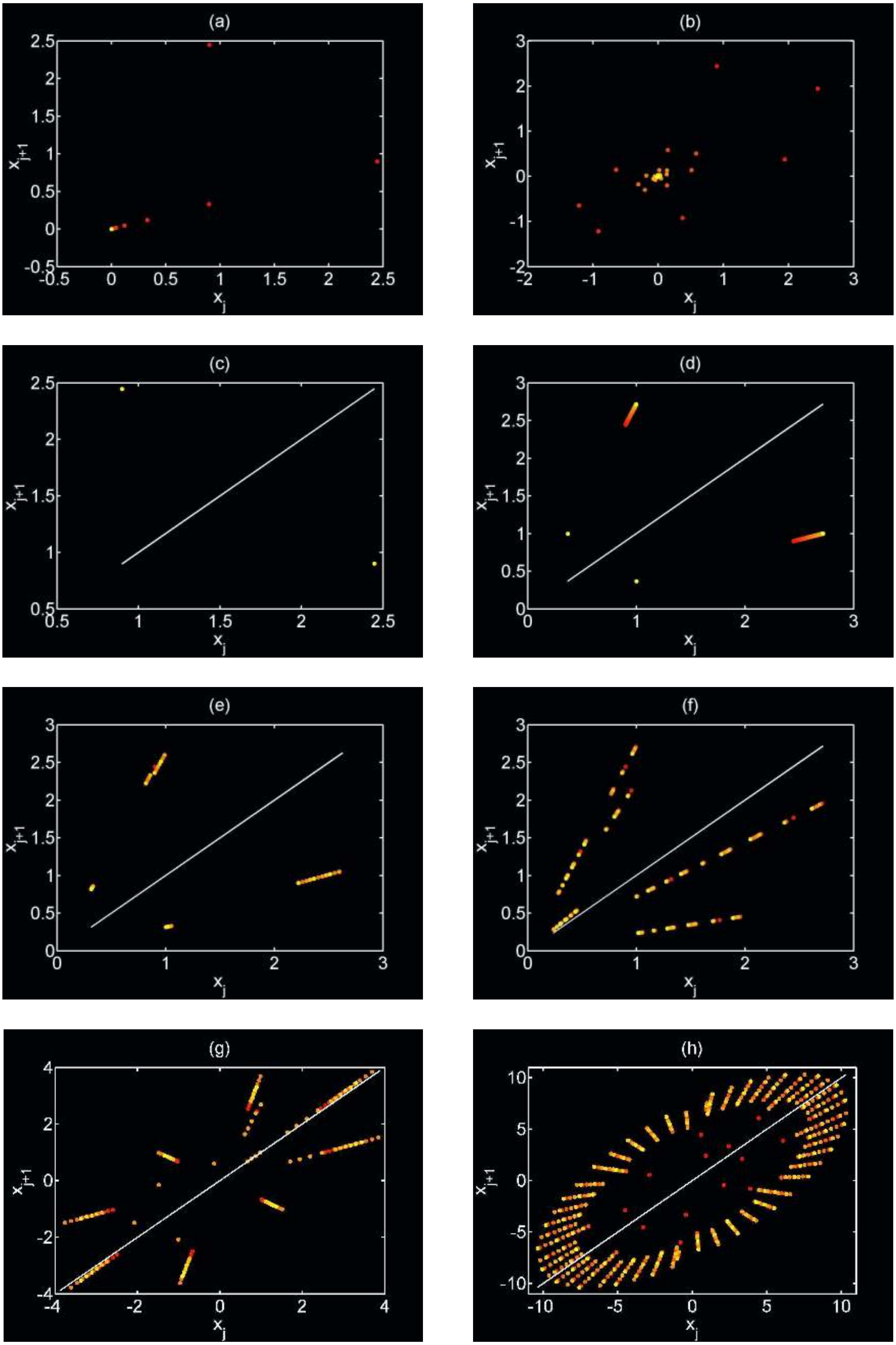

Fig. 3. Set of results for $a = 10$, $P = 13.6788$ and $\tau_s = 0.1$, iteration starts with red, ends with yellow, (a) $\tau_p = 0$, $\Phi(x_j) \equiv x_j$, (b) $\tau_p = 2 \cdot 10^{-2}$, $\Phi(x_j) \equiv x_j$, (c) $\tau_p = 0$, (d) $\tau_p = 10^{-6}$, (e) $\tau_p = 10^{-3}$, (f) $\tau_p = 10^{-2}$, (g) $\tau_p = 2 \cdot 10^{-2}$, (h) $\tau_p = 3.13 \cdot 10^{-2}$.

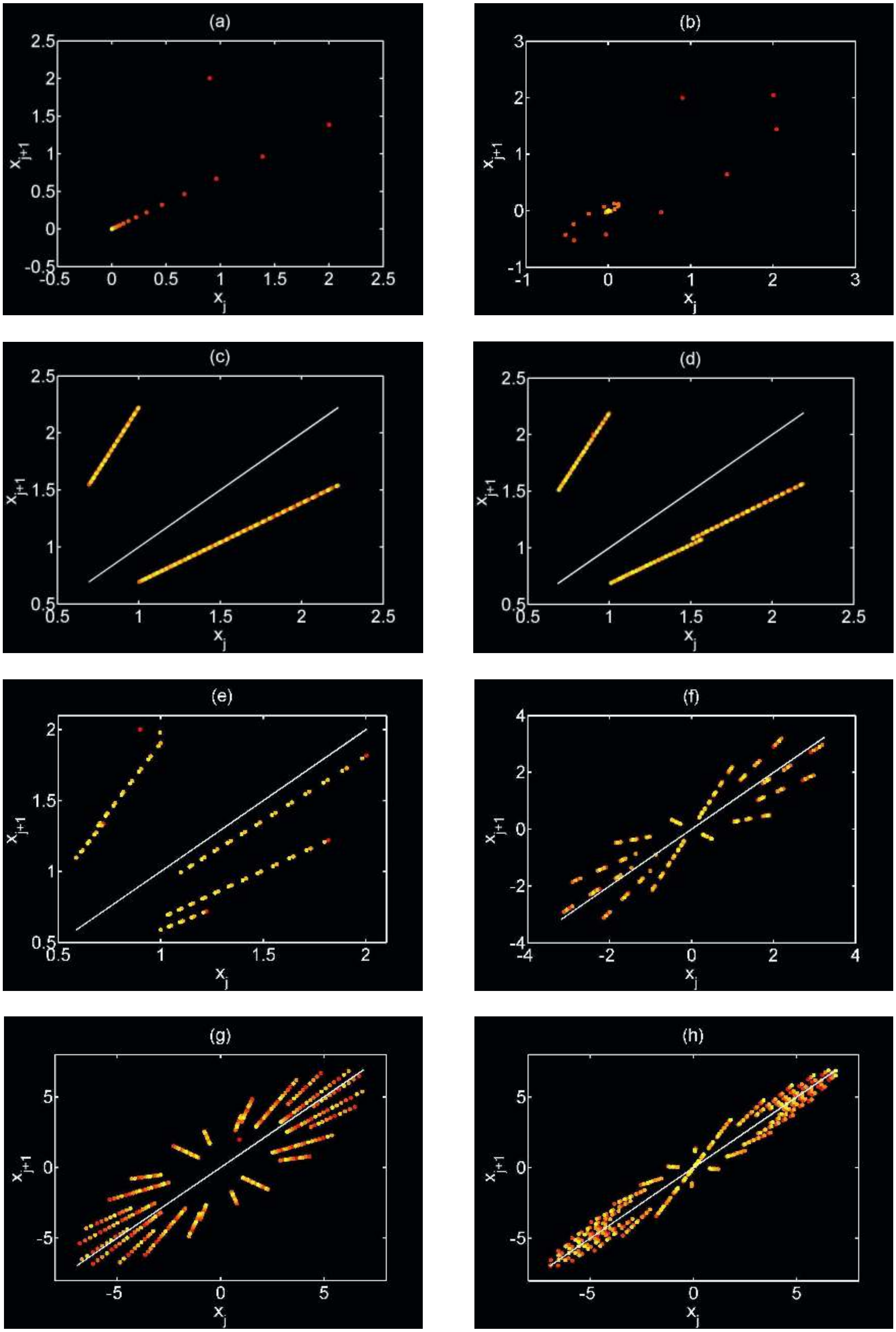

Fig. 4. (a)–(g) Set of results for $a = 8$, $P = 10$ and $\tau_s = 0.1$, iteration starts with red, ends with yellow, (a) $\tau_p = 0$, $\Phi(x_j) \equiv x_j$, (b) $\tau_p = 3 \cdot 10^{-2}$, $\Phi(x_j) \equiv x_j$, (c) $\tau_p = 0$, (d) $\tau_p = 10^{-3}$, (e) $\tau_p = 10^{-2}$, (f) $\tau_p = 4 \cdot 10^{-2}$, (g) $\tau_p = 5.57 \cdot 10^{-2}$, (h) $a = 8$, $P = 8.4444$, $\tau_s = \tau_p = 0.0802$ (i.e. $A = 1.9$, $B = 0.95$, $C = 0$).

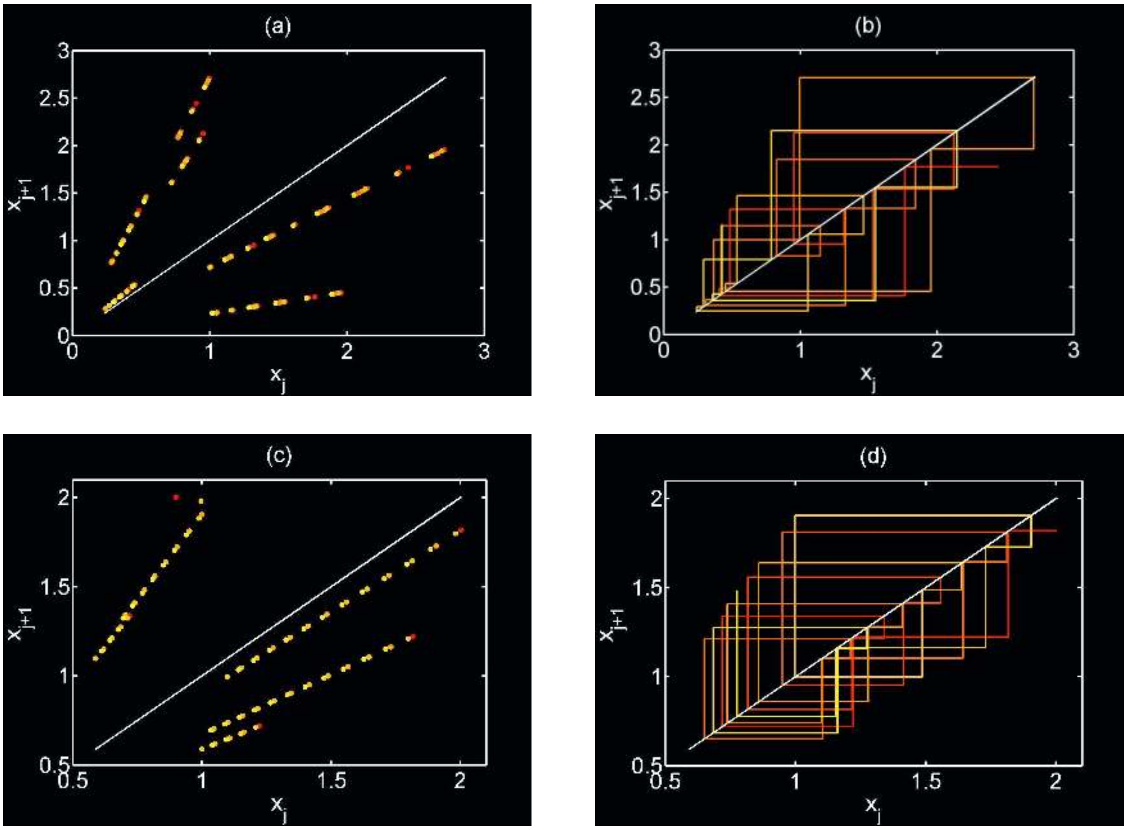

Fig. 5. The map and the stair step diagram, iteration starts with red, ends with yellow, (a) and (b) $a = 10$, $P = 13.6788$, $\tau_s = 0.1$ and $\tau_p = 10^{-2}$, (c) and (d) $a = 8$, $P = 10$, $\tau_s = 0.1$ and $\tau_p = 10^{-2}$.

near the border of the stability domain to present a very complicated motion. Note that a small change in the parameters can affect where points appear in the figure.

Numerical results for $a = 10$, $P = 13.6788$, $\tau_s = 0.1$, $\tau_p = 0.01$ as well as $a = 8$, $P = 10$, $\tau_s = 0.1$, $\tau_p = 0.01$ are repeated in Fig. 5 and the corresponding stairstep diagrams for the first couple of steps are associated. The stairstep diagrams show the consecutive steps. There are five and four lines in Figs. 5(a) and 5(c), respectively, where points of orbits are situated. It can be seen that a point in a particular line is mapped into another but usually the same line. However, this regularity is broken when the orbit is in the neighborhood of 1.

4. Conclusions

Some mechanical problems, as gear pairs with backlash [Kollár *et al.*, 2003; Lóránt & Stépán, 1996; Theodossides & Natsiavas, 2000], may be described by bilinear discontinuous maps. When these mechanical elements are used in a driving system of a digitally controlled machine, the equations of motion can be reduced to piecewise linear discrete maps. In particular, we examine the dynamics of the typical scalar map (1). The domain where stable motion can be obtained is determined and we consider the parameter domain given by the stability conditions. The map has the following properties in this parameter domain. Its only fixed point is the origin which is unstable. The set $[A - B, A)$ (or $(-A, -(A - B)]$ or their union) is an invariant set. If condition (8) is satisfied, then every orbit is eventually periodic, otherwise orbits can be described as follows

- every orbit is dense in $\mathcal{A}$,
- orbits have sensitive dependence on initial conditions on $\mathcal{A}$,
- the Lyapunov exponents of orbits are 0 and
- orbits have quasiperiodic subsequences.

We also examined the map arising from a more realistic model which includes processing delay. The obtained motions appear more complicated and the analysis of the resulting dynamics is more tedious, but the numerical results predict similar properties (density, sensitive dependence on initial conditions, 0 Lyapunov exponent and quasiperiodic subsequences) as the orbits have in case of the scalar map (1).

Since there exists a positively invariant, indecomposable attractive set $\mathcal{A}$, and the map has sensitive dependence on initial conditions as well as topological transitivity due to the density of orbits on the attractor, this motion could be called chaotic in the sense of Wiggins [1990]. However, orbits have quasiperiodic subsequences and the sensitive dependence is very weak as given in Remark 2.6, so the motion is not unpredictable. Also, the positive Lyapunov exponent required for a chaotic motion in [Alligood *et al.*, 1996] does not exist here. Consequently, the typical motions of this relevant set of digitally controlled systems with backlash can be more complicated than quasiperiodic, but they are not classified as chaotic according to the definition of a chaotic attractor in [Alligood *et al.*, 1996].

Acknowledgments

The authors gratefully thank Dr. Tamás Tél for his illuminating discussions and valuable advice. This research was supported by the Hungarian National Science Foundation under Grant No. OTKA T043368/03.

References

Alligood, K. T., Sauer, T. D. & Yorke, J. A. [1996] *Chaos: An Introduction to Dynamical Systems* (Springer-Verlag, NY).

Collet, P. & Eckmann, J.-P. [1980] *Iterated Maps on the Interval as Dynamical Systems* (Birkhäuser, Boston).

Devaney, R. L. [1989] *An Introduction to Chaotic Dynamical Systems* (Addison-Wesley).

Haller, G. & Stépán, G. [1996] "Micro-chaos in digital control," *J. Nonlin. Sci.* **6**, 415–448.

Kollár, L. E. [2001] *Dynamics of Digitally Controlled Unstable Mechanical Systems*, PhD thesis, Department of Applied Mechanics, Budapest University of Technology and Economics, Budapest, Hungary.

Kollár, L. E., Stépán, G. & Turi, J. [2003] "Dynamics of delayed piecewise linear systems," *Fifth Mississippi State Conf. Differential Equations and Computational Simulations, Electronic J. Differential Equations*, Conference 10, pp. 163–185; http://ejde.math.swt.edu or http://ejde.math.unt.edu

Lóránt, G. & Stépán, G. [1996] "The role of nonlinearities in the dynamics of a single railway wheelset," *Mach. Vibr.* **5**, 18–26.

Szépfalusy, P. & Tél, T. [1982] *A Káosz, The Chaos* (Akadémiai Kiadó, Budapest) (in Hungarian).

Theodossides, S. & Natsiavas, S. [2000] "Nonlinear dynamics of gear-pair systems with periodic stiffness and backlash," *J. Sound Vibr.* **229**, 287–310.

Wiggins, S. [1990] *Introduction to Applied Nonlinear Dynamical Systems and Chaos* (Springer-Verlag, NY).